

1 **Enantiomeric fractionation during biotransformation of chiral pharmaceuticals in**
2 **recirculating water-sediment test flumes**

3 Jonas Mechelke^{1,2}, Dominique Rust^{1,3}, Anna Jaeger^{4,5}, Juliane Hollender^{1,2*}

4

5 ¹ Eawag, Swiss Federal Institute of Aquatic Science and Technology, 8600 Dübendorf, Switzerland

6 ² Institute of Biogeochemistry and Pollutant Dynamics, ETH Zurich, 8092 Zürich, Switzerland

7 ³ Department of Chemistry, University of Zurich, 8057 Zürich, Switzerland

8 ⁴ Department Ecohydrology, Leibniz-Institute of Freshwater Ecology and Inland Fisheries, Berlin, Germany

9 ⁵ Geography Department, Humboldt University Berlin, Berlin, Germany

10

11 * Corresponding Author

12

13

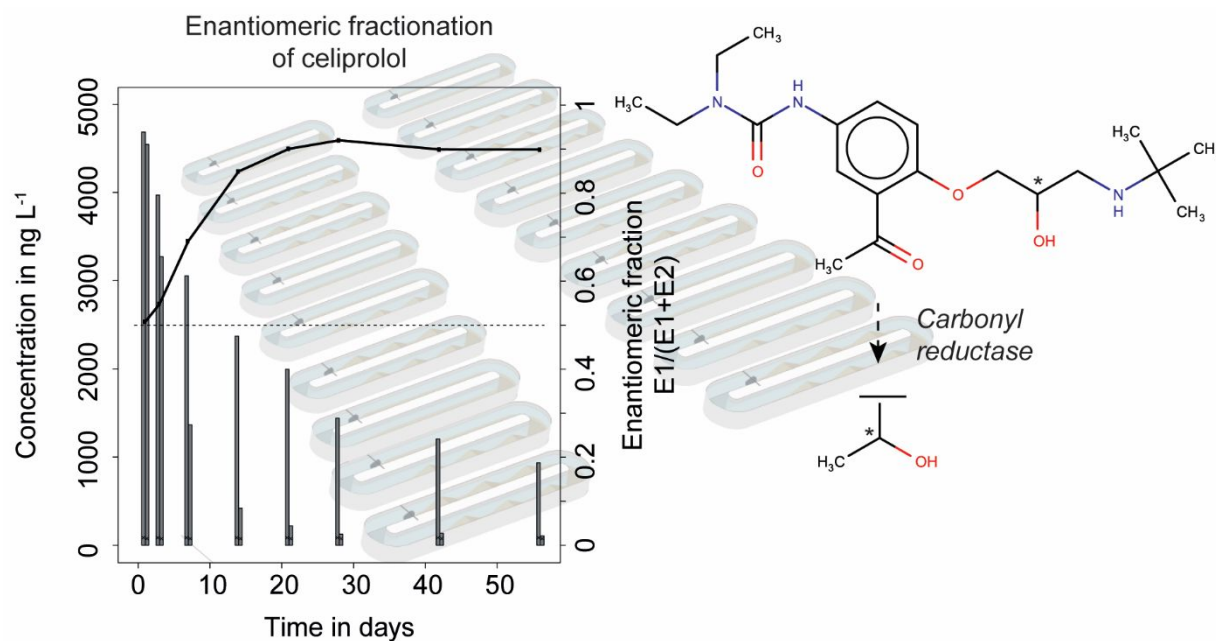
14

This document is the accepted manuscript version of the following article:
Mechelke, J., Rust, D., Jaeger, A., & Hollender, J. (2020). Enantiomeric fractionation during biotransformation of chiral pharmaceuticals in recirculating water-sediment test flumes. Environmental Science and Technology. <https://doi.org/10.1021/acs.est.0c00767>

Abstract

Many organic contaminants entering the aquatic environment feature stereogenic structural elements that give rise to enantiomerism. While abiotic processes usually act identical on enantiomers, biotic processes, such as biodegradation often result in enantiomeric fractionation (Efr), i.e. the change of the relative abundance of enantiomers. Therefore, EFr offers the opportunity to differentiate biodegradation in complex environmental systems from abiotic processes. In this study, an achiral-chiral two-dimensional liquid chromatographic method for the enantioseparation of selected pharmaceuticals was developed. This method was then applied to determine the enantiomeric compositions of 8 chiral pharmaceuticals in 20 water-sediment test flumes and test EFr as an indicator of biodegradation. While all 8 substances were attenuated by at least 60%, 5 (atenolol, metoprolol, celiprolol, propranolol, flecainide) displayed EFr. No EFr was observed for citalopram, fluoxetine and venlafaxine despite almost complete attenuation (80 to 100%). Celiprolol, a barely studied beta-blocker, revealed the most distinct EFr among all investigated substances, however, EFr varied considerably with biodiversity. Celiprolol-H2 was identified as a biological transformation product, possibly formed by reduction of the celiprolol keto group through a highly regio- and enantioselective carbonyl reductase. While celiprolol-H2 was observed across all flumes, as expected, its formation was faster in flumes with high bacterial diversity where also EFr was highest. Overall, EFr and transformation product formation together served as good indicators of biological processes; however, the strong dependence of EFr on biodiversity limits its usefulness in complex environmental systems.

Graphical abstract



35 1 Introduction

36 Pharmaceuticals and pesticides are common environmental organic contaminants (OCs) that are constantly
37 emitted into the aquatic environment through treated or untreated wastewater and agriculture [1]. The majority of
38 newly released drugs (72% between 2001 and 2010) [2], and a significant share of the pesticides in use (about
39 30%) are chiral [3], i.e. they possess stereogenic structural elements (e.g., a stereogenic center) that give rise to
40 enantiomerism. Enantiomers are stereoisomers that feature the same connectivity among atoms but differ in their
41 spatial arrangement. While abiotic processes (e.g. sorption, hydrolysis, abiotic oxidation-reduction, photo
42 transformation, dilution) usually act identical on enantiomers, biotic processes, such as biotransformation
43 (including: OC uptake, transport, translocation, biodegradation, enzymatic isomerization) often happen to result in
44 enantiomeric fractionation (EFr), i.e. the change of the relative abundance of enantiomers. Therefore, EFr is often
45 used to differentiate biodegradation in complex environmental systems from abiotic processes. EFr during biotic
46 processes can be explained by the different interactions of enantiomers with chiral environments in natural
47 molecules, for example in enzymes ("chiral catalysts") due to chiral amino acids (mostly L-amino acids), or in DNA,
48 RNA or ribozymes due to chiral ribose or deoxyribose [4–8]. Biotic processes might also proceed without EFr (e.g.
49 [9–11]), i.e. enzymes are not strictly stereospecific [12], and rarely enantioselective abiotic processes have been
50 reported (e.g. [13–16]). Biotic processes without EFr are conceivable if the enantioselective step of a
51 biotransformation cascade (e.g. binding to the active site of an enzyme or activation) is not rate determining, or if
52 the OC-enzyme interaction or the transformation (or both) do not involve (or occur far-off) the stereogenic element
53 [12]. By contrast, enantioselective abiotic processes might occur, where a chiral pollutant interacts with chiral
54 environments of e.g. sludge [13], soil [14], dissolved organic carbon [16], or minerals [14, 15]. Therefore, other
55 indicators of biotic processes such as biological transformation products (TPs) play a crucial role when the EFr of
56 a chiral OC is investigated.

57 Deriving EFr from the enantiomeric composition of an OC requires the separation of its enantiomers. Indirect
58 separation methods rely on derivatization of enantiomers (identical physicochemical properties in achiral
59 environments) with chiral reagents into diastereomers. Diastereomers have distinct physicochemical properties in
60 achiral environments and therefore can often be separated on common achiral liquid or gas chromatographic
61 stationary phases. Direct methods proceed without derivatization and use liquid, supercritical fluid or gas
62 chromatographic separation on chiral stationary phases. Less conventional is the gas phase separation of
63 enantiomers by ion-mobility spectrometry [17]. Chiral liquid chromatography (LC) is most widespread for the direct
64 analysis of (semi-)polar chiral OC in aqueous samples [18, 19], however, only few multi-residue methods exist,
65 which typically allow for the enantioseparation of still a small number of structurally similar OCs. Chiral LC uses
66 chiral stationary phases with chiral selectors immobilized on solid support (usually porous silica). A universal chiral
67 stationary phase for the multi-residue analysis of OCs does not exist, however, a few specific stationary phases,
68 such as immobilized polysaccharides, proteins and macrocyclic glycopeptide antibiotics [19, 20] are widely used.
69 In particular vancomycin-based stationary phases have proven capable of resolving a wide range of
70 environmentally relevant OCs [21–23]. The latter stationary phases are multi-modal, i.e. the same column can be
71 operated in multiple chromatographic separation modes by manipulating the composition of the mobile phase.
72 Examples are polar ionic mode (PIM, polar organic solvent with small amounts of acid and base or salt), reversed-
73 phase mode (RPM, polar organic solvent with water or aqueous buffer), polar organic mode (POM, polar organic
74 solvent without mobile phase additive) or normal phase mode (NOM, non-polar organic solvent with polar solvent
75 modifiers) [24]. Depending on the respective mode, separation might be more or less prone to interferences by
76 sample matrix (e.g. polar ions), which is typically removed by offline solid-phase extraction prior to chiral LC.
77 Another approach is achiral-chiral two-dimensional liquid chromatography (2DLC) column-switching, where the first
78 LC dimension serves the online sample clean-up (through e.g. size exclusion or trap-and-elute) and the second
79 dimension is a chiral LC column for the resolution of enantiomers [25, 26]. Eluent compatibility in both dimensions
80 is crucial for the 2DLC approach. In this study, we aimed to develop an achiral-chiral 2DLC column-switching
81 electrospray ionization high-resolution tandem mass spectrometry (achiral-chiral 2DLC-ESI-HRMS/MS) multi-
82 residue method for the enantiomeric resolution of 40 OCs in complex water samples. The most suitable method
83 was successfully applied to 8 chiral OCs (atenolol, metoprolol, celiprolol, propranolol, flecainide, citalopram,
84 fluoxetine, venlafaxine) in the surface water (SW) of 20 recirculating water-sediment test flumes over a period of
85 56 days. All selected pollutants featured a single chiral carbon atom as the stereogenic element and were initially

spiked to the test flumes as racemic mixtures (equal amounts of the 2 possible enantiomers). The flume experimental design [27, 28], the fate of all 30 spiked OCs, and a comprehensive screening of suspected biological TPs [29] are provided in detail elsewhere. The present study focusses on the development of the chiral LC method and its subsequent application to investigate the fate of 8 chiral OCs at the enantiomer level.

2 Materials and Methods

2.1 Chemicals

Details on racemic reference standards (STDs) and isotope-labeled internal standards (IS) used during analytical method development, instrumental analysis and for the fortification of test flumes are provided in the supplementary information (SI.A). Acetic acid (100%, anhydrous for analysis), formic acid (98-100%) and ammonium acetate (for analysis) were obtained from Merck (Germany). 2-butanol (p.a., ≥99.5%), ammonia (4 mol L⁻¹ in methanol) and propionic acid (p.a., ≥99.5%) were purchased from Sigma-Aldrich (Germany or Switzerland). Methanol (LC/MS grade, Optima™) was supplied by Fisher Scientific (Switzerland). NANOpure™ water (NPW) was generated using a lab water purification system (D11911, Barnstead/Thermo Scientific, USA).

2.2 One-dimensional chiral liquid chromatography: substance selection, method development and validation

For the development of a (one-dimensional, 1D) chiral LC method, 32 chiral pharmaceuticals of different therapeutic classes, 5 chiral pesticides, 2 illicit drugs and 1 personal care product were initially selected (SI.A). Selection criteria were (i) occurrence at River Erpe (Berlin, Germany), a wastewater effluent-impacted stream and joint field site within the European Marie-Curie training network HypoTRAIN [30–32], (ii) the same stereogenic element among OCs, i.e. a single chiral carbon atom, resulting in a manageable number of 2 enantiomers per substance, and (iii) availability of racemic STDs and ISs. The 40 OCs were largely ionized at pH 7 (7 anions, 16 cations, 4 zwitterions, 13 neutral) and covered a wide range of polarity ($\log D_{\text{ow,pH7}} = -6.2$ to 4.5), molecular weight (159 to 501 Da), and substance classes (see above). Enantiomeric separation was tested with a vancomycin-based Astec Chirobiotic™ V column (150 mm length x 2.1 mm I.D., 5 μm particles, Sigma-Aldrich, Switzerland) equipped with an Astec Chirobiotic™ V guard column (20 mm length x 4 mm I.D., 5 μm particles, Sigma-Aldrich, Switzerland). The column was operated in a column oven (Mistral, Spark, Netherlands) with an adjustable temperature range between 10 and 90 °C. The Chirobiotic™ V column was selected since it had proven suitable for enantiomeric multi-residue separations of a wide range of chiral aquatic contaminants (mostly pharmaceuticals) [21–23, 33–35]. Although the Chirobiotic™ V column can be operated in PIM, RPM, POM or NOM (see above) [24], in this work, only PIM and RPM were extensively optimized for the enantiomeric resolution of the selected OCs. POM and NOM were hardly compatible with ESI-MS and selected analytes, and were therefore not further pursued. In PIM, different organic solvents, i.e. mostly alcohols of varying polarity (MeOH, EtOH, IPA, MeCN, rac 2-butanol), were tested with different mobile phase additives (ammonium acetate/formate, acetic/formic/propionic acid, ammonia). In RPM, the same organic solvents as in PIM were used with some added proportion of aqueous buffer. Method development resulted in 4 final chiral LC methods (Table 1). The method that allowed for the separation of the largest number of OCs in a single analytical run was validated with and without a sample enrichment step for NPW and 3 environmental matrices, i.e., SW, effluent wastewater (EWW), and influent wastewater (IWW). In the workflow without sample enrichment (referred to as ‘direct’ workflow), sample centrifugation (2 mL sample, 3,020 g, 30 min, 20°C, Megafuge 1.0R, Heraeus) was followed by IS addition (80 ng mL⁻¹) to a 1 mL supernatant aliquot and aqueous large-volume injection (50 μL) into the chiral column. Details of the second workflow based on sample enrichment by vacuum-assisted evaporative concentration (VEC, concentration factors: 150 for SW, 37.5 for EWW and 15 for IWW) are described in [36]. None of the sample preparations included a clean-up step. Details on the instrumental analysis can be found in the SI.E.

2.3 Two-dimensional achiral-chiral 2DLC column-switching electrospray ionization high-resolution tandem mass spectrometry

To ensure applicability of 1DLC (cf. Table 1) to water samples (artificial EWW-dominated SW) from recirculating water-sediment test flumes, an achiral-chiral 2DLC-ESI-HRMS/MS method was established (details on method development in SI.D.a; a scheme of the column-switching approach is shown in Fig. SI.D-7). Inspired by achiral-chiral 2DLC using octyl restricted-access media bovine serum albumin column in the first dimension (achiral), and chiral LC in the second dimension [25, 26], in the present study the achiral dimension was a reversed-phase column (Atlantis T3, 20 mm length x 3 mm I.D., 5 μ m particles, Waters, Switzerland), which served the purpose of analyte retention and online sample clean-up (removal of matrix interferences that affect chromatographic enantiomer separation and have ions that could interfere in PIM). The second dimension was the aforementioned vancomycin-based chiral column. Detection was achieved by HRMS/MS interfaced to chiral LC by an ESI interface that was operated in positive ion mode (see Table SI.E-7 for details). Suspected biological TPs of atenolol, metoprolol, celiprolol, fluoxetine and propranolol tentatively identified in a former study on an achiral LC column [29] were further investigated in this study by manually extracting ion chromatograms acquired by achiral-chiral 2DLC-ESI-HRMS/MS for deriving hints on their enantiomeric composition.

2.4 Flume experiments

The flume experimental design [27], the flume hydrology [28] and the biotransformation of OCs [29] have been described in detail elsewhere. In brief, the major variables among the recirculating water-sediment test flumes were bacterial diversity and hyporheic exchange flow. Both were established at 3 levels (high, medium, low) by dilution (S1: 10^{-1} , S3: 10^{-3} , S6: 10^{-6}) of river sediment with baked commercial sand (bacterial diversity) and by different numbers of bedforms (B6, B3, B0) in the flume sediment (hyporheic flow), respectively. Combinations of the 2 variables resulted in 9 treatments. All treatments were set up as duplicates, but the mid-level (S3+B3) in 4 replicates. After a pre-incubation period of 12 days to reach same bacterial abundances, flumes were fortified with 31 OCs at $10 \mu\text{g L}^{-1}$, of which 16 were spiked at racemic composition. SW was sampled 1, 3, 7, 14, 21, 28, 42 and 56 days after fortification, and for analytical reasons, only 8 of the 16 racemic OCs were finally analyzed. While the flumes were inside a white tent to shield them from weather, block direct solar radiation and reduce the influence of photolysis, air-borne microbial contamination was possible at any time [27].

3 Results and discussion

3.1 Four one-dimensional chiral liquid chromatographic methods for the enantiomeric resolution of 20 chiral organic pollutants

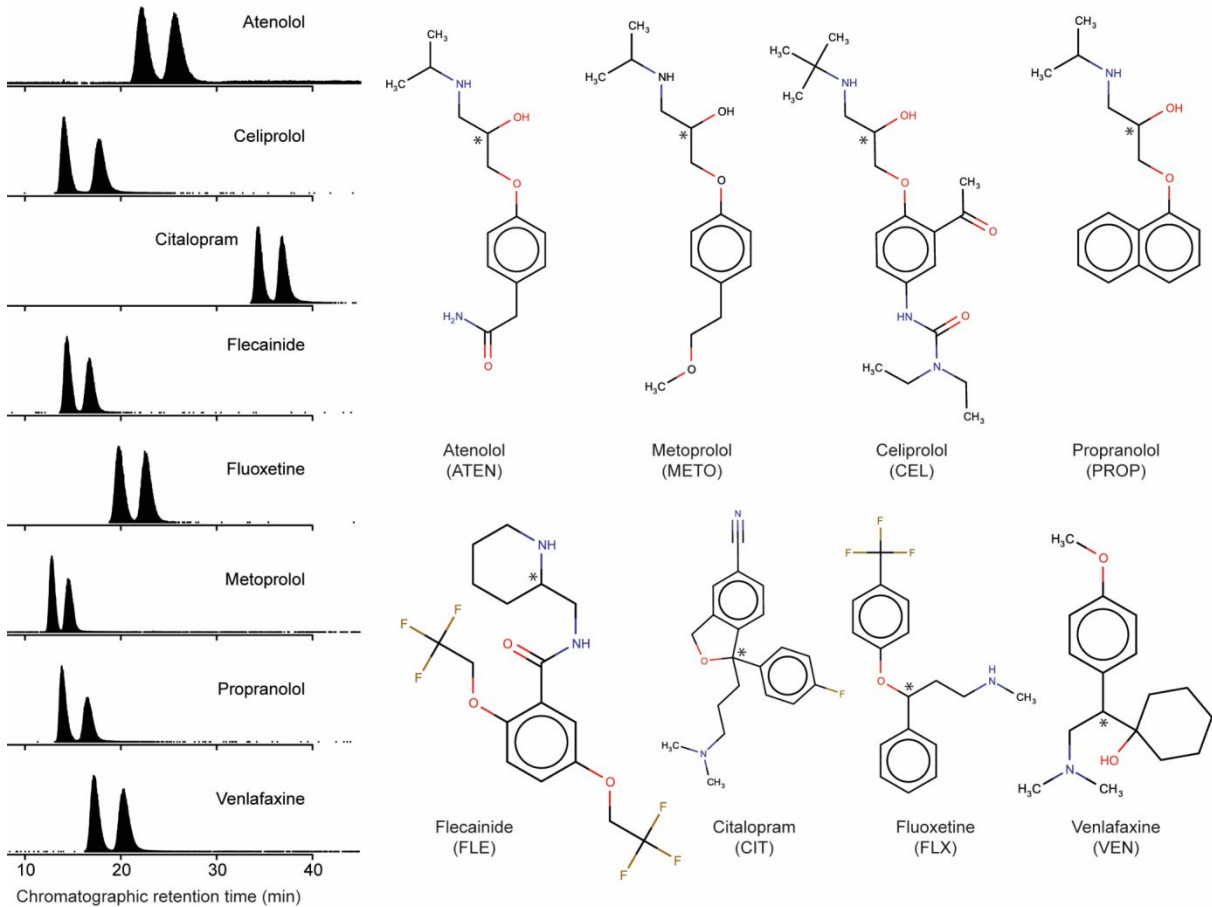
More than 500 optimization runs (test parameters: mobile phase composition, flow rate, separation temperature) resulted in 4 final multi-residue methods (2 in PIM, 2 in RPM) that allowed for the simultaneous separation of up to 10 OCs (method 1) and 20 OCs in total (Table 1). The limited number of resolved enantiomers was an expected outcome, which can be attributed to the high selectivity of chiral stationary phases. Three column oven (separation) temperatures (10, 20 and 30 $^{\circ}\text{C}$) were tested and a lower temperature typically improved the enantiomeric resolution (a comparison between 10 and 30 $^{\circ}\text{C}$ is provided in SI.C.c). Therefore, all final methods were run at 10 $^{\circ}\text{C}$. As a general observation, enantiomers of structurally similar OCs (drugs of the same therapeutic class) were resolved with the same chiral LC method (Table 1), e.g. beta-blockers (atenolol, celiprolol, metoprolol, propranolol, occasionally sotalol, all having secondary or tertiary amines) with method 1, profens (ketoprofen, ibuprofen) by method 3, and benzamide antipsychotics (amisulpride, sulpiride) with method 4 (enantiomeric separation shown in SI.B). Method 1 was able to resolve the largest number of racemic OCs and was therefore validated with and without sample enrichment (see section 2.2 for details and SI.C for validation parameters). Enantiomeric separation of benproperine and sotalol (method 1) was occasionally lost, even in the absence of matrix (i.e., in NPW). The other 8 OCs with constant enantiomeric resolution ($R_s > 1.0$, definition of R_s in SI C.b) in NPW (both workflows) are depicted in Fig. 1. Since none of the two workflows involved a sample clean-up, enantiomeric resolution of individual OCs either decreased in environmental samples (SW, EWW, IWW) compared to NPW, or was entirely lost (exemplarily shown for EWW in Fig. 2, see Fig. SI.D-8 for IWW and SW). Loss of enantiomeric resolution was

176 especially pronounced in concentrated samples (VEC in Fig. 2 and Fig. SI.D-8), likely due to the enrichment of
177 matrix constituents alongside analytes causing matrix effects on the chiral stationary phase and thus loss of
178 chromatographic resolution in PIM (cf. SI.D.d). The desired peak resolution was ≥ 1 , i.e. a maximum overlap of
179 2.3% between peaks of Gaussian distribution. In NPW, peak resolutions were > 1.5 (0.15% overlap) and ranged
180 from 1.5 (fluoxetine) to 2.1 (celiprolol). In spiked EWW, peak resolutions were 0.8 (atenolol), 1.1 (venlafaxine) and
181 1.4 (citalopram), in spiked IWW 1 (atenolol), 1.3 (venlafaxine) and 1.5 (citalopram) (other OCs <LOQ). Matrix
182 interferences, i.e. in this case matrix-induced signal enhancement and suppression, were also reflected in LOQs,
183 which ranged from 100 to 1'000 ng L⁻¹ in NPW (median: 375 ng L⁻¹), and were shifted towards higher values in SW
184 (95 to 1'200 ng L⁻¹, median: 400 ng L⁻¹), EWW (100 to 2'200 ng L⁻¹, median: 500 ng L⁻¹), and IWW (100 to 1'700 ng
185 L⁻¹, median: 500 ng L⁻¹). (details on calculation in SI.C.a and individual values in Table SI.C-4).

187 **Table 1** Four final (one-dimensional) chiral liquid chromatographic methods for the enantiomeric resolution of 20
188 chiral analytes (all analytes are drugs except the herbicide bromacil). Separation temperature: 10°C. Analytes in
189 brackets: no constant enantiomeric resolution in NPW ($R_s<1.0$).

Method	Eluent; separation mode	Flow rate in mL min ⁻¹ (flow duration)	Column post-rinse (solvent)	Enantioresolved analytes
1	5 mM NH ₃ /HOAc (1:3, v/v) in MeOH; PIM	0.4 (30 min), 1.2 (15 min)	15 min, 0.8 mL min ⁻¹ (eluent)	atenolol, (benproperine), celiprolol, citalopram, flecainide, fluoxetine, metoprolol, propranolol, (sotalol), venlafaxine
2	1 mM NH ₃ /propionic acid (1:2, v/v) in NPW/ MeOH/butan-2-ol (95:5:5, v/v/v); RPM	0.1 (50 min)	MeOH	bromacil, metaxalone, methsuximide
3	10 mM NH ₄ OAc in NPW/MeOH (50:50, v/v); RPM	0.1 (12 min)	MeOH/NPW (70:30, v/v) & MeOH	etodolac, ketoprofen, naproxen, methotrexate, ibuprofen
4	1 mM NH ₄ OAc in MeOH, 0.05% formic acid; PIM	0.1 (30 min)	MeOH/NPW (70:30, v/v) & MeOH	amisulpride, sulpiride

190 HOAc: acetic acid. MeOH: methanol. NH₄OAc: ammonium acetate. NPW: NANOpure™ water. PIM/RPM: polar ionic/reversed-phase mode



191
192 **Fig. 1** Eight chiral drugs with constant enantiomeric resolution ($R_s>1.0$) in NANOpure™ water using method 1
193 (Table 1). *Left*: extracted ion chromatograms of analytes (sum of enantiomers: 10 $\mu\text{g L}^{-1}$, absolute: 0.5 ng, no
194 enrichment).

3.2 Achiral-chiral two-dimensional liquid chromatography ensures enantiomeric resolution in complex water matrices

The achiral-chiral 2DLC approach with the validated method 1 in the second LC dimension functioned without extensive optimization and enantiomeric resolution was successfully restored for racemic analytes that were unresolved in complex (concentrated) samples using 1D chiral LC (cf. section 3.1). This is shown in Fig. 2 for racemic STD and IS in EWW (concentrated and not concentrated, other matrices in Fig. SI.D-8). Other than that, the successful application of the 2DLC method to a flume water sample (0 bedforms, low bacterial diversity, 1 day after fortification with racemic STD) is shown.

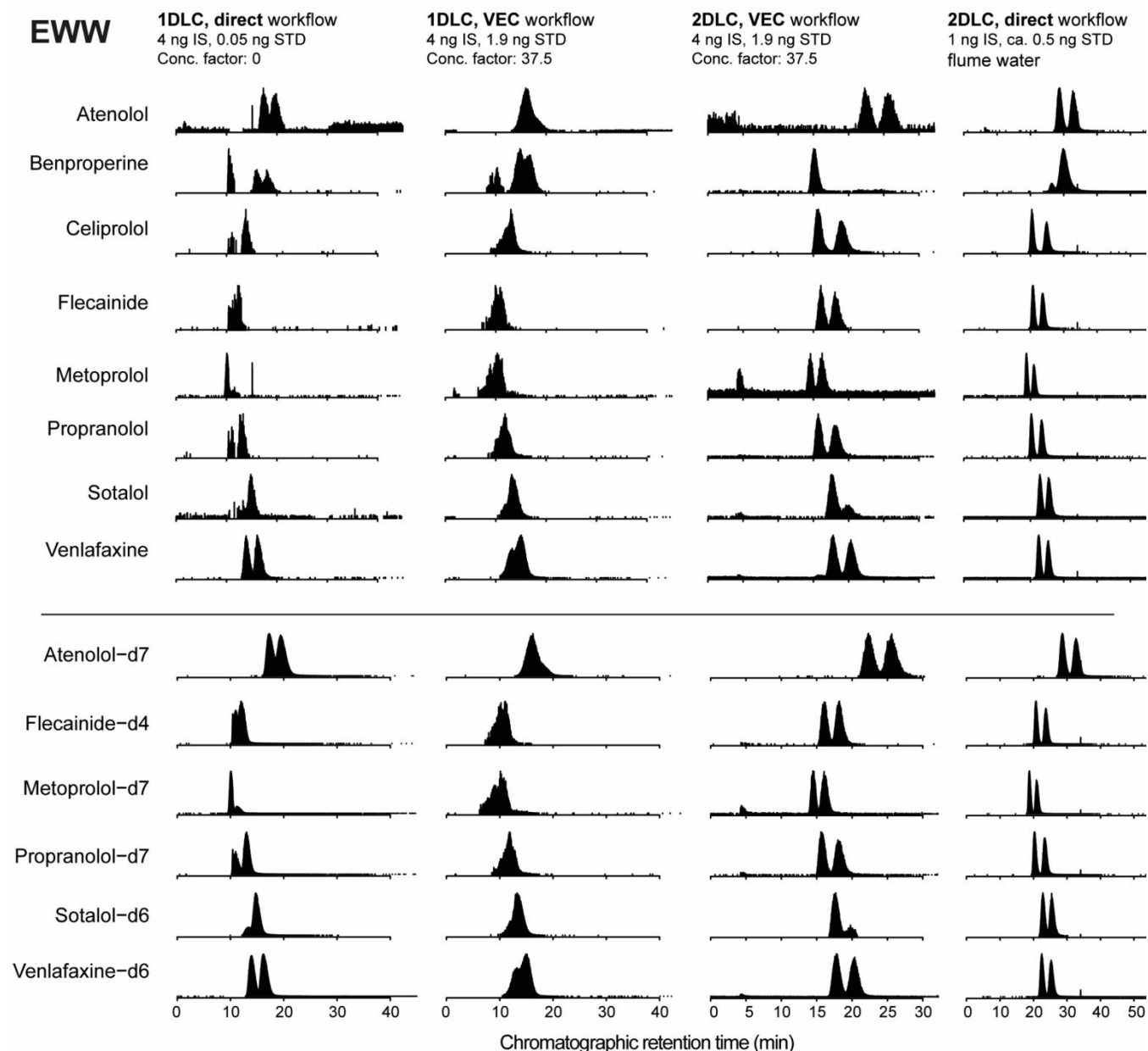
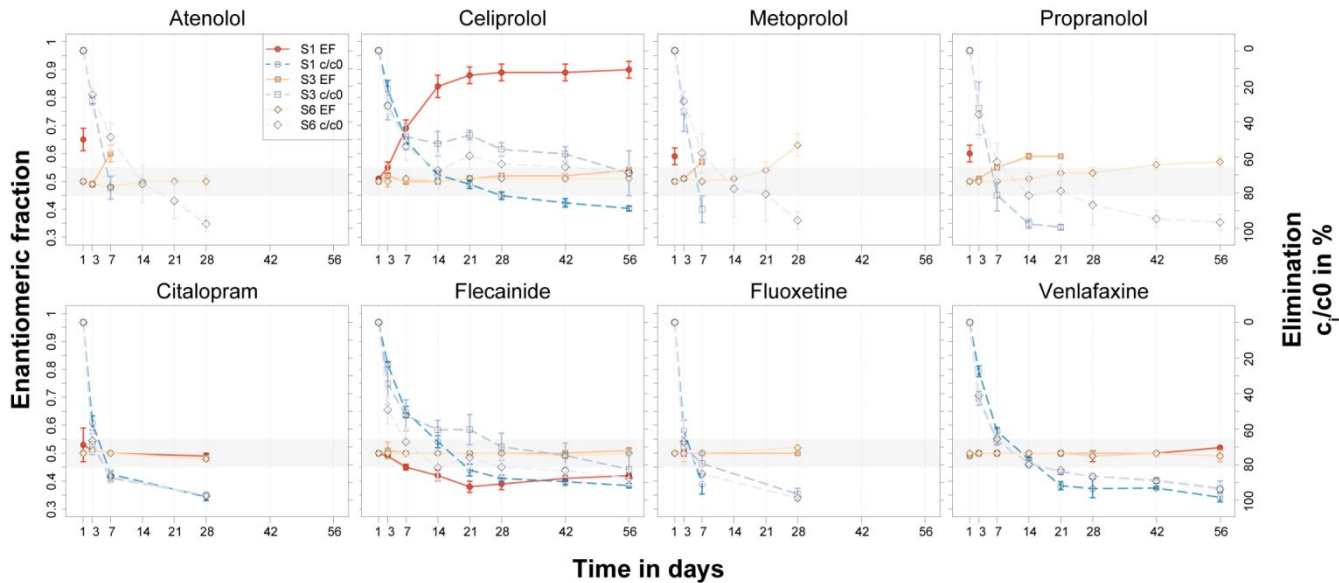


Fig. 2 Loss or decrease of enantiomeric resolution during one-dimensional chiral liquid chromatography (1DLC, 1st and 2nd column, in comparison to NPW in Fig. 1) of racemic analyte standards (STD, top) and assigned racemic isotope-labelled internal standards (IS, bottom) in effluent wastewater (EWW) and EWW concentrated by vacuum-assisted evaporation (VEC) – restoration of enantiomeric resolution through achiral-chiral two-dimensional liquid chromatography (2DLC, 3rd column) and its application to an artificial EWW sample taken from a recirculating water-sediment test flume (4th column). *General notes:* analyte amounts in column header are the sum of both enantiomers; scaling of omitted y-axes can differ; STDs and isotope-labeled internal standards of citalopram and

211 fluoxetine are not shown (for other matrices see Fig. SI.D-8) due to analytical issues; mass traces cut after 50 min
212 in 4th column.

213 **3.3 Enantiomeric composition of 8 chiral pharmaceuticals over 56 days in recirculating water-sediment**
214 **test flumes**

215 The 2DLC approach was used to determine enantiomeric compositions (in this study presented as the enantiomeric
216 fraction EF, i.e., the concentration of E1 divided by the sum concentration of E1+E2; E1: first eluting enantiomer,
217 E2: second eluting enantiomer) of 8 chiral OCs in river-simulating water-sediment test flumes over 56 days (Fig. 3,
218 SI.F to SI.H). During the analysis of flume SW, EFs of calibration standards were measured at the beginning and
219 end of a 2DLC sequence, serving as a quality control. All OCs were eliminated by at least 60% in all 20 flumes
220 (atenolol/citalopram/fluoxetine/metoprolol: complete elimination, celiprolol/flecainide/propranolol: ≥61%,
221 venlafaxine: ≥89%). Compound-specific half-lives (sum of enantiomers, assuming first-order kinetics [27]) ranged
222 from <0.5 d (mostly S1) to 24 d (celiprolol in S3+B3). Significantly different enantiomer-specific half-lives were only
223 observed at most distinct EF (0.93 for celiprolol in S1 flumes, E1: 16 to 18 days, E2: 4.5 to 5.6 days, see SI.J and
224 SI.K for details). EFr in this study refers to the change of the initial EF of 0.50±0.05 (racemic) to an EF greater or
225 smaller 0.50±0.05. Fig. 2 depicts EFs and elimination percentages of 8 chiral OCs over the 56-days experimental
226 period after fortification. While attenuation of citalopram, fluoxetine and venlafaxine was not accompanied by EFr,
227 metoprolol and propranolol displayed EFr in the majority of treatments (EF >0.55). Atenolol, celiprolol and flecainide
228 underwent treatment-specific EFr, of which only for flecainide an EF <0.45 was observed. A dependency between
229 EFr and elimination percentage did not become apparent within 56 days.



230
231 **Fig. 3** Enantiomeric fractions (EF, solid lines) and elimination (dashed lines) of 8 chiral organic contaminants over
232 the 56-days experimental period. Treatments differ in sediment dilution (i.e. bacterial diversity; S1, S3, S6). Bedform
233 numbers are not resolved. Contaminants were spiked at racemic composition (EF 0.50±0.05, grey bar). Data points
234 with error bars: mean±SD. The maximum EF over 56 days are summarized in SI.I.

235 **3.3.1 Unchanged enantiomeric compositions of citalopram, fluoxetine and venlafaxine**

236 Citalopram, fluoxetine and venlafaxine underwent complete attenuation (venlafaxine >80%) across all flumes, but
237 without distinct EFr (only minor changes within 0.5±0.05). This is in line with biodegradation studies conducted at
238 similar test conditions, i.e. attenuation in river water simulating microcosms (fluoxetine) [37] or EWW-receiving
239 rivers (all 3 OCs) [38] was accompanied by only mild or no EFr. By contrast, attenuation in activated sludge
240 simulating microcosms [37, 38] was typically more complete and accompanied by EFr. These behaviors were
241 reflected in profiled wastewaters (IWW, EWW), i.e. citalopram was typically found at non-racemic EF between 0.57
242 (IWW) and 0.7 (EWW) [21], fluoxetine at around 0.2 (IWW) [21] and 0.7 (EWW) [39–41], and venlafaxine mostly at

racemic composition [34, 41–44]. In fate studies at the enantiomer level (e.g. [37, 38]), some TPs of the above OCs were monitored, however, attempts were barely made to explain the underlying pathways leading to EFr. A comprehensive screening for citalopram TPs in activated sludge was performed in [45]. Some of the reported TPs (citalopram carboxylic acid/desmethyl/didesmethyl) were occasionally found in the flumes, but without a distinct pattern. [29] Biological TPs (zebrafish metabolites) and photodegradation products of fluoxetine were recently described in [46]. Norfluoxetine, the major biological TP of fluoxetine, was not observed in flume SW [29]. 4-trifluoromethylphenol, a later generation target TP of fluoxetine, was only found in single flumes (no general pattern). [29] In some S1 treatments (B6 and B3), N-succinyl fluoxetine was tentatively identified [29] (confidence level [47]: 3, also found as biological TP in zebrafish [46] and in activated sludge [48]). Venlafaxine target TPs monitored in flumes were O-desmethyl/N-desmethyl/N,N-didesmethyl/N,O-didesmethylvenlafaxine and venlafaxine-N-oxide, of which only the N-oxide and N-desmethyl TP demonstrated clear formation patterns over time (other TPs were mostly <LOQ). Despite these TP findings, biotransformation was not reflected in EFs, which remained virtually constant.

3.3.2 Enantiomeric fractionation of atenolol, metoprolol, celiprolol, propranolol and flecainide

Celiprolol is a barely studied beta-blocker that showed the most distinct EFr among all substances and an interesting enantioselective behavior, indicating biodegradation at highest bacterial diversity (Fig. 3, S1, EF of 0.9). Also at low and medium bacterial diversity, celiprolol underwent attenuation, however, without significant EFr (small changes within 0.5 ± 0.05). EFr of atenolol and metoprolol, both beta-blockers that are structurally similar to celiprolol (Fig. 1), was significantly lower (between 0.55 and 0.7). In a former biodegradation study using activated sludge simulating microcosms [49], slight enantioselectivity was observed for metoprolol, whereas atenolol degraded non-enantioselectively. In another study [50], EFr of metoprolol was observed along a river stretch (0.49 at site A, 0.43 at site B), with further EFr across the water-sediment interface (<0.40). In wastewaters, atenolol [21–23, 33, 41, 51] and metoprolol [21–23, 51] were mainly racemic (0.50 ± 0.05), with the EFs of atenolol and metoprolol ranging from 0.39 (IWW) [51] to 0.55 (EWW) [33], and 0.3 [41] to 0.60 [51] (both IWW), respectively. A common (and major) TP of atenolol and metoprolol (and other structurally similar beta-blockers) [52] is atenolol (metoprolol) acid. It is formed from atenolol by (enzymatic) hydrolysis [53], e.g. in cyanobacteria [54], or abiotically [55], and by dealkylation of metoprolol (aerobic biotransformation and human metabolism [56, 57], microalgae [54, 58], fungi [59]). In the test flumes, atenolol/metoprolol acid emerged at medium and low bacterial diversity (S3, S6), where it was further attenuated (details in [29]): the lower the bacterial diversity (the higher the sediment dilution), the slower was its further attenuation. At highest bacterial diversity (across all bedform levels), atenolol/metoprolol acid was only observed in single replicates, and, if at all, only in the first couple days after fortification [29]. In the respective treatments, its further attenuation was presumably so fast, that formation-attenuation dynamics were not captured with the chosen sampling resolution. Thus, while EFr of atenolol/metoprolol indicated biodegradation at highest bacterial diversity (S1), absence (or fast degradation) of atenolol/metoprolol acid among these treatments would not necessarily have allowed this conclusion. In the case of atenolol/metoprolol, parent attenuation, EFr, and TP formation combined provided meaningful evidence of biotransformation.

Propranolol underwent EFr in all treatments apart from treatment S3+B6 (cf. SI.I). This is in line with former biodegradation studies (activated sludge simulating microcosms), in which propranolol underwent enantioselective degradation (racemic to 0.43 and 0.44 in [60], minor EFr in [49]). Naphthoxyacetic acid (reported in [61] as human metabolite) was the only propranolol TP tentatively identified in a suspect screening of flume SW [29]. Its formation followed a similar pattern as atenolol/metoprolol acid, i.e. fast formation was followed by fast attenuation at highest bacterial diversity (S1). At intermediate diversity (S3), formation and attenuation were both slower and at lowest diversity (S6), only formation and the onset of attenuation after approx. 56 days were observed [29]. EFr during biotransformation of propranolol to naphthoxyacetic acid appears feasible, since the transformation occurs at the chiral side chain and the chiral center itself (loss of chirality).

Flecainide concentrations decreased by at least 60% across all flumes, however, distinct EFr was only observed at highest bacterial diversity (all S1 flumes). Unlike the other 4 OCs that demonstrated preferential degradation of E2, E1 was preferentially degraded in case of flecainide (enrichment of E2). Major metabolites formed in human metabolism (m-O-dealkyl-flecainide, m-O-dealkyl-flecainide lactam, phenolic glucuronide and sulfate conjugates of the latter) [62] were not detected in flume SW [29]. Flecainide is marketed as racemate (equipotent enantiomers)

[63] and approx. 10 to 50% of this drug are excreted unchanged by non-enantioselective renal pathways [62]. To our knowledge, EFr of flecainide has only been reported during nonrenal clearance (metabolism) from humans with hepatic cytochrome P4501D6 deficiency [64], but not during microbial (bacterial) biodegradation.

3.3.3 Celiprolol-H2 – structural evidence for a reduced celiprolol transformation product

The strong EFr of celiprolol in S1 flumes (Fig. 3) might be explained by enzymatic reduction of the acetyl group to yield celiprolol-H2, a transformation that can be highly regio- and enantioselective [65–67]. Enantioselective reduction at environmental conditions has been described before. For instance, the chiral drug climbazole has been reported to undergo enantioselective reduction to climbazole-H2 at biotic anoxic conditions in constructed wetlands and batch sludge experiments [68]. The proposed mechanism was carbonyl reductase catalyzed ketone reduction by direct hydride transfer from the NAD(P)H cofactor. In flume SW, oxygen levels at days 28, 36, 44 and 86 were significantly different in different sediment dilutions, i.e. they were lowest in S1 flumes, followed by S3 and S6 [27]. Consequently, reductive processes were most favored in S1 flumes.

A signal at the mass of celiprolol-H2 evolved in all treatments [29], however, it evolved faster at highest bacterial diversity, e.g. in S1 treatments after 1 day (extracted-ion chromatograms of celiprolol and celiprolol-H2 obtained by chiral analysis are shown in Fig. 4 for some selected flumes, celiprolol-H2 time-trends of the suspect screening can be found in [29]). In all other treatments, the respective signal evolved after a lag-phase of approx. 3 weeks [29]. EFrs at low and medium bacterial diversity (S3, S6) were in the 0.5 ± 0.05 range, except for a slight enrichment of E1 in one of the replicate S3+B0 treatments. The rather moderate EFr of atenolol and metoprolol in comparison to celiprolol might be due to other biotransformation pathways that involve less stereospecific enzymes. Moreover, sites of transformation in the parent molecules are the primary amide group in atenolol and the methyl ether moiety in metoprolol. Both groups are opposite (*para*) the chiral center, i.e. more distant than acetyl group and chiral center in celiprolol (*ortho*). We previously tentatively identified celiprolol-H2 based on the exact mass at a confidence level of identification of 4 (no MS2 information) [29]. Re-analysis of flume SW increased the confidence level to 2 (diagnostic MS2 fragments). For further (unambiguous) structural confirmation (confidence level 1), samples were compared (Fig. 4, *bottom*) against a celiprolol-H2 reference standard that was synthesized by the reduction of celiprolol with aluminium borohydride (details in SI.J.a). In this process of suspect identification, celiprolol-H2 was also identified as an impurity of the celiprolol reference material (analytical grade). Consequently, it is possible that minute amounts of celiprolol-H2 were added during flume fortification with celiprolol, however, the strong EFr of celiprolol and the concentration decrease of celiprolol accompanied by the signal increase of celiprolol-H2 rather prove biotic formation processes. Moreover, EFr of celiprolol was also reflected in the stereoisomeric composition of celiprolol-H2 (Fig. 4, *top*), which is further strong evidence for the proposed transformation reaction (enantioselective enzymatic reduction). For S1+B0 flumes a significant higher formation of only one celiprolol-H2 diastereomer was observed, whereas for S3+B3 flumes both diastereomers were formed in similar amounts in accordance with the enantioselective and non-enantioselective transformation of celiprolol, respectively. In general, literature information on celiprolol TPs and human metabolites is hardly existent (e.g. [69]), which might be explained by its minor metabolization (1-3%) in the human body [70] or its lower prescription and use compared to other beta-blockers (e.g. [71]). This study provides the first clear evidence for a celiprolol TP that is likely to be formed under environmental conditions.

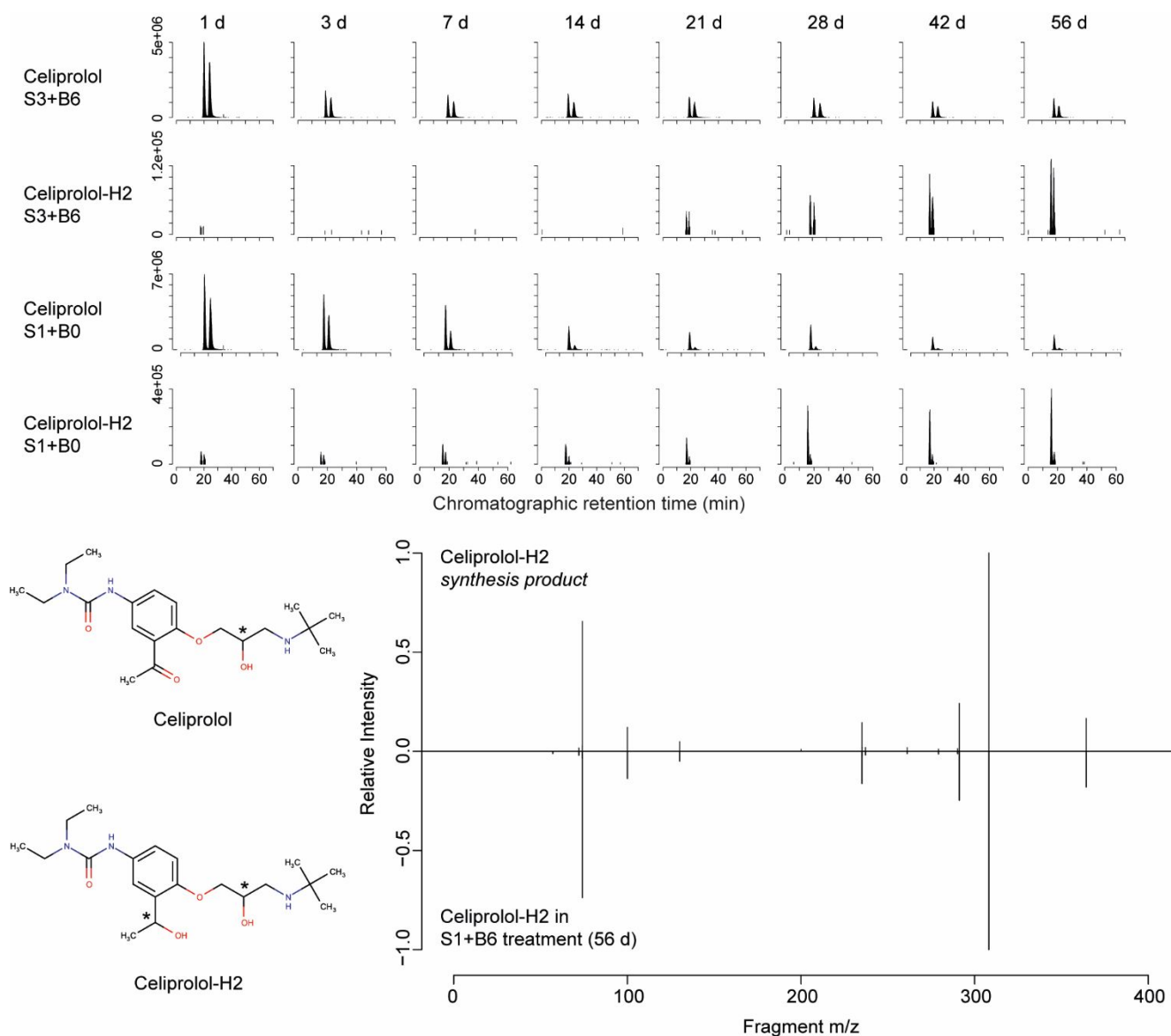


Fig. 4 Evidence for the (biotic) enzymatic reduction of celiprolol to celiprolol-H2. *Top*: Extracted-ion chromatograms (2DLC) of celiprolol and celiprolol-H2 from 1 d to 56 d after fortification. At intermediate bacterial diversity (S3+B6) celiprolol attenuation and celiprolol-H2 formation occur via a non-enantioselective process. At high bacterial diversity (S1+B0), celiprolol undergoes strong enantiomeric fractionation and only 1 dominant celiprolol-H2 peak evolves (please note: the enantiomeric composition of celiprolol-H2 was assessed visually). *Bottom*: head-to-tail plot of ms2 fragments obtained for synthesized celiprolol-H2 and celiprolol-H2 in a S1+B6 flume. 96% similarity between ms2 spectra at 10 ppm mass tolerance and 0.01 relative intensity cut-off (overlap: 14 of 16 fragments).

4 Environmental implications

The development of a multi-residue method for the enantioseparation of chemically diverse chiral OCs in a single analytical run was time intense and more complex than expected. This is attributable to the method development process, which is generally often based on trial and error. Further separation might only be reached with other chiral stationary phases providing different interactions. Method development ultimately revealed that most OCs with similar chemical structures can be separated within the same analytical run. However, chiral separation was often lost during direct chiral analysis of OCs in environmental samples due to matrix interferences. Consequently, elimination of matrix components is essential to achieve enough resolving power in enantiomeric analysis. In our study this could be solved by achiral-chiral 2DLC column-switching, a fast and efficient method implementing the sample clean-up into the analytical run.

Application of 2DLC to water-sediment test flumes revealed that EFr can be affected by the level of bacterial diversity. An example is the strong EFr of celiprolol at high bacterial diversity, which was virtually absent at middle and low diversity. Similar trends were found for atenolol and flecainide. Since biodiversity and, thus, the variety of enzymatic pathways is expected to vary across environmental compartments and conditions, such as redox conditions for celiprolol, the usefulness of EFr as indicator of biological processes seems limited. This statement is supported by the different EFs of the beta-blockers atenolol and metoprolol reported for various environmental compartments in the literature (cf. section 3.3.2). The combination of EFr with transformation product analysis can solve this dilemma by providing an additional indicator. In the case of celiprolol, 2DLC did not only provide first evidence on its enantioselective degradation, it also gave important hints at the formation of celiprolol-H2. In this context, parent attenuation, TP formation and EFr were complementary indicators of biodegradation. While it has been shown that bacterial diversity and sediment bedforms can significantly influence the dissipation half-lives of OCs in water-sediment test flumes [29], chiral analysis further revealed that a dissipation half-life can also depend on the enantiomeric composition of a test compound. For a better comparison of dissipation half-lives in fate studies, efforts should be made to report the stereoisomeric compositions of test chemicals.

5 Acknowledgements

We thankfully acknowledge Prof. Dr. Laurent Bigler (University of Zurich) for supervising the master thesis of Dominique Rust. Furthermore, we thank all HypoTRAIN ESRs, guest PhD students (Anne Mehrtens, University of Oldenburg; Andrea Portmann, Colorado School of Mines), Phillip Blaen (University of Birmingham) and supervisors that were involved in the flume experiment. Special thanks go to the Environmental Change Outdoor Laboratory (University of Birmingham), Dr. Samuel Derrer and Febin Ambalathattil (both Eawag Dübendorf) for the synthesis of celiprolol-H2, and Dr. Daniel Rentsch (Empa Dübendorf) for structural confirmation of celiprolol and celiprolol-H2 by NMR. Finally, we gratefully acknowledge ChemAxon Ltd. for the donation of the academic research license to the JChem package.

6 Funding

This project has received funding from the European Union's Horizon 2020 research and innovation programme under the Marie Skłodowska-Curie grant agreement No 641939 and the Swiss State Secretariat for Education, Research and Innovation.

7 Conflicts of Interest

The authors declare that they have no known competing financial interests or personal relationships that could have appeared to influence the work reported in this paper.

8 References

1. aus der Beek T, Weber F-A, Bergmann A, Hickmann S, Ebert I, Hein A, Küster A (2016) Pharmaceuticals in the environment--Global occurrences and perspectives. *Environ Toxicol Chem* 35:823–835 . doi: 10.1002/etc.3339
2. Agranat I, Wainshtein SR, Zusman EZ (2012) The predicated demise of racemic new molecular entities is an exaggeration. *Nat Rev Drug Discov* 11:972–973 . doi: 10.1038/nrd3657-c1
3. Jeschke P (2018) Current status of chirality in agrochemicals. *Pest Manag Sci* 74:2389–2404 . doi: 10.1002/ps.5052
4. Clayden J, Greeves N, Warren S (2012) Stereochemistry. In: *Organic Chemistry*, 2nd ed. Oxford University Press
5. Clayden J, Greeves N, Warren S (2012) Asymmetric synthesis. In: *Organic Chemistry*, 2nd ed. Oxford University Press
6. Clayden J, Greeves N, Warren S (2012) Organic chemistry of life. In: *Organic Chemistry*, 2nd ed. Oxford University Press
7. Smith SW (2009) Chiral toxicology: It's the same thing only different. *Toxicol. Sci.* 110:4–30
8. Klebe G (2005) Differences in binding of stereoisomers to protein active sites. *Supramol Struct Funct* 8 31–52 . doi: 10.1007/0-306-48662-8_3
9. Ribeiro AR, Maia AS, Moreira IS, Afonso CM, Castro PML, Tiritan ME (2014) Enantioselective quantification of fluoxetine and norfluoxetine by HPLC in wastewater effluents. *Chemosphere* 95:589–596 . doi: 10.1016/j.chemosphere.2013.09.118
10. Tan H, Cao Y, Tang T, Qian K, Chen WL, Li J (2008) Biodegradation and chiral stability of fipronil in aerobic and flooded paddy soils. *Sci Total Environ* 407:428–437 . doi: 10.1016/j.scitotenv.2008.08.007
11. Chen M, He Y, Yang Y, Huang L, Zhang H, Ye Q, Wang H (2017) Non-stereoselective transformation of the chiral insecticide cycloxyaprid in aerobic soil. *Sci Total Environ* 579:667–674 . doi: 10.1016/j.scitotenv.2016.11.043
12. Buchholz K, Kasche V, Bornsheuer UTT (2005) Basics of enzymes as biocatalysts. In: *Introduction to Enzyme Technology*, 2nd ed. WILEY-VCH, pp 33–110
13. Sanganyado E, Fu Q, Gan J (2016) Enantiomeric selectivity in adsorption of chiral β -blockers on sludge. *Environ Pollut* 214:787–794 . doi: 10.1016/j.envpol.2016.04.091
14. Gámiz B, Facenda G, Celis R (2016) Evidence for the effect of sorption enantioselectivity on the availability of chiral pesticide enantiomers in soil. *Environ Pollut* 213:966–973 . doi: 10.1016/j.envpol.2016.03.052
15. Hazen RM, Filley TR, Goodfriend GA (2001) Selective adsorption of L- and D-amino acids on calcite: Implications for biochemical homochirality. *Proc Natl Acad Sci U S A* 98:5487–5490 . doi: 10.1073/pnas.101085998
16. Qiao X, Carmosini N, Li F, Lee LS (2011) Probing the primary mechanisms affecting the environmental distribution of estrogen and androgen isomers. *Environ Sci Technol*. doi: 10.1021/es200073h
17. Dwivedi P, Wu C, Matz LM, Clowers BH, Siems WF, Hill HH (2006) Gas-phase chiral separations by ion mobility spectrometry. *Anal Chem* 78:8200–8206 . doi: 10.1021/ac0608772
18. Pe S (2008) Applications of LC-MS to quantitation and evaluation of the environmental fate of chiral drugs and their metabolites. 27: . doi: 10.1016/j.trac.2008.09.003
19. Petrie B, Camacho-Muñoz D, Castrignanò E, Evans S, Kasprzyk-Hordern B (2015) Chiral Liquid Chromatography Coupled with Tandem Mass Spectrometry for Environmental Analysis of Pharmacologically Active Compounds. *LCGC Eur* 28:151 . doi: 10.2174/1573411012666151009195039
20. Evans SE, Kasprzyk-Hordern B (2014) Applications of chiral chromatography coupled with mass spectrometry in the analysis of chiral pharmaceuticals in the environment. *Trends Environ Anal Chem* 1:e34–e51 . doi: 10.1016/j.teac.2013.11.005
21. MacLeod SL, Sudhir P, Wong CS (2007) Stereoisomer analysis of wastewater-derived β -blockers, selective serotonin re-uptake inhibitors, and salbutamol by high-performance liquid chromatography-tandem mass spectrometry. *J Chromatogr A* 1170:23–33 . doi: 10.1016/j.chroma.2007.09.010

- 431 22. Bagnall JP, Evans SE, Wort MT, Lubben a. T, Kasprzyk-Hordern B (2012) Using chiral liquid
432 chromatography quadrupole time-of-flight mass spectrometry for the analysis of pharmaceuticals and illicit
433 drugs in surface and wastewater at the enantiomeric level. *J Chromatogr A* 1249:115–129 . doi:
434 10.1016/j.chroma.2012.06.012
- 435 23. López-Serna R, Kasprzyk-Hordern B, Petrović M, Barceló D (2013) Multi-residue enantiomeric analysis of
436 pharmaceuticals and their active metabolites in the Guadalquivir River basin (South Spain) by chiral liquid
437 chromatography coupled with tandem mass spectrometry. *Anal Bioanal Chem* 405:5859–5873 . doi:
438 10.1007/s00216-013-6900-7
- 439 24. Astec (2004) Chirobiotic Handbook, 5th ed
- 440 25. Barreiro JC, Vanzolini KL, Cass QB (2011) Direct injection of native aqueous matrices by achiral-chiral
441 chromatography ion trap mass spectrometry for simultaneous quantification of pantoprazole and
442 lansoprazole enantiomers fractions. *J Chromatogr A* 1218:2865–2870 . doi: 10.1016/j.chroma.2011.02.064
- 443 26. Barreiro JC, Vanzolini KL, Madureira TV, Tiritan ME, Cass QB (2010) A column-switching method for
444 quantification of the enantiomers of omeprazole in native matrices of waste and estuarine water samples.
445 *Talanta* 82:384–391 . doi: 10.1016/j.talanta.2010.04.056
- 446 27. Jaeger A, Coll C, Posselt M, Mechelke J, Rutere C, Betterle A, Raza M, Mehrtens A, Meinikmann K,
447 Portmann A, Singh T, Blaen P, Krause S, Horn M, Hollender J, Benskin J, Sobek A, Lewandowski J (2019)
448 Using recirculating flumes and a response surface model to investigate the role of hyporheic exchange and
449 bacterial diversity on micropollutant half-lives. *Environ Sci Process Impacts*. doi: 10.1039/c9em00327d
- 450 28. Betterle A, Jaeger A, Posselt M, Coll C, Benskin J, Schirmer M (2019) Analysis of hyporheic exchange
451 fluxes in recirculating flumes under heterogeneous microbial and morphological conditions. *ESPI in prep.*:
- 452 29. Posselt M, Mechelke J, Rutere C, Coll C, Jaeger A, Raza M, Meinikmann K, Krause S, Sobek A,
453 Lewandowski J, Horn MA, Hollender J, Benskin JP (2020) Bacterial Diversity Controls Transformation of
454 Wastewater-Derived Organic Contaminants in River-Simulating Flumes. *Environ Sci Technol*. doi:
455 10.1021/acs.est.9b06928
- 456 30. Jaeger A, Posselt M, Betterle A, Schaper J, Mechelke J, Coll C, Lewandowski J (2019) Spatial and Temporal
457 Variability in Attenuation of Polar Organic Micropollutants in an Urban Lowland Stream. *Environ Sci Technol*
458 53:2383–2395 . doi: 10.1021/acs.est.8b05488
- 459 31. Posselt M, Jaeger A, Schaper JL, Radke M, Benskin JP (2018) Determination of polar organic
460 micropollutants in surface and pore water by high-resolution sampling-direct injection-ultra high performance
461 liquid chromatography-tandem mass spectrometry. *Environ Sci Process Impacts* 20:1716–1727 . doi:
462 10.1039/c8em00390d
- 463 32. Mechelke J, Vermeirssen ELM, Hollender J (2019) Passive sampling of organic contaminants across the
464 water-sediment interface of an urban stream. *Water Res*. doi: 10.1016/j.watres.2019.114966
- 465 33. MacLeod SL, Wong CS (2010) Loadings, trends, comparisons, and fate of achiral and chiral
466 pharmaceuticals in wastewaters from urban tertiary and rural aerated lagoon treatments. *Water Res*
467 44:533–544 . doi: 10.1016/j.watres.2009.09.056
- 468 34. Gasser G, Pankratov I, Elhanany S, Werner P, Gun J, Gelman F, Lev O (2012) Field and laboratory studies
469 of the fate and enantiomeric enrichment of venlafaxine and O-desmethyivenlafaxine under aerobic and
470 anaerobic conditions. *Chemosphere* 88:98–105 . doi: 10.1016/j.chemosphere.2012.02.074
- 471 35. Ribeiro AR, Afonso CM, Castro PML, Tiritan ME (2013) Enantioselective HPLC analysis and biodegradation
472 of atenolol, metoprolol and fluoxetine. *Environ Chem Lett* 11:83–90 . doi: 10.1007/s10311-012-0383-1
- 473 36. Mechelke J, Longrée P, Singer H, Hollender J (2019) Vacuum-assisted evaporative concentration combined
474 with LC-HRMS/MS for ultra-trace-level screening of organic micropollutants in environmental water
475 samples. *Anal Bioanal Chem* 411:2555–2567 . doi: 10.1007/s00216-019-01696-3
- 476 37. Andrés-Costa MJ, Proctor K, Sabatini MT, Gee AP, Lewis SE, Pico Y, Kasprzyk-Hordern B (2017)
477 Enantioselective transformation of fluoxetine in water and its ecotoxicological relevance. *Sci Rep* 7: . doi:
478 10.1038/s41598-017-15585-1
- 479 38. Evans S, Bagnall J, Kasprzyk-Hordern B (2017) Enantiomeric profiling of a chemically diverse mixture of
480 chiral pharmaceuticals in urban water. *Environ Pollut* 230:368–377 . doi: 10.1016/j.envpol.2017.06.070
- 481 39. Barclay VKH, Tyrefors NL, Johansson IM, Pettersson CE (2011) Trace analysis of fluoxetine and its

- metabolite norfluoxetine. Part I: Development of a chiral liquid chromatography-tandem mass spectrometry method for wastewater samples. *J Chromatogr A* 1218:5587–5596 . doi: 10.1016/j.chroma.2011.06.024
40. Barclay VKH, Tyrefors NL, Johansson IM, Pettersson CE (2012) Trace analysis of fluoxetine and its metabolite norfluoxetine. Part II: Enantioselective quantification and studies of matrix effects in raw and treated wastewater by solid phase extraction and liquid chromatography-tandem mass spectrometry. *J Chromatogr A* 1227:105–114 . doi: 10.1016/j.chroma.2011.12.084
41. Evans SE, Davies P, Lubben A, Kasprzyk-Hordern B (2015) Determination of chiral pharmaceuticals and illicit drugs in wastewater and sludge using microwave assisted extraction, solid-phase extraction and chiral liquid chromatography coupled with tandem mass spectrometry. *Anal Chim Acta* 882:112–126 . doi: 10.1016/j.aca.2015.03.039
42. Castrignanò E, Lubben A, Kasprzyk-Hordern B (2016) Enantiomeric profiling of chiral drug biomarkers in wastewater with the usage of chiral liquid chromatography coupled with tandem mass spectrometry. *J Chromatogr A* 1438:84–99 . doi: 10.1016/j.chroma.2016.02.015
43. Kasprzyk-Hordern B, Kondakal VVR, Baker DR (2010) Enantiomeric analysis of drugs of abuse in wastewater by chiral liquid chromatography coupled with tandem mass spectrometry. *J Chromatogr A* 1217:4575–4586 . doi: 10.1016/j.chroma.2010.04.073
44. Kasprzyk-Hordern B, Baker DR (2012) Enantiomeric profiling of chiral drugs in wastewater and receiving waters. *Environ Sci Technol* 46:1681–1691 . doi: 10.1021/es203113y
45. Beretsou VG, Psoma AK, Gago-Ferrero P, Aalizadeh R, Fenner K, Thomaidis NS (2016) Identification of biotransformation products of citalopram formed in activated sludge. *Water Res* 103:205–214 . doi: 10.1016/j.watres.2016.07.029
46. Tisler S, Zindler F, Freeling F, Nödler K, Toelgyesi L, Braunbeck T, Zwiener C (2019) Transformation Products of Fluoxetine Formed by Photodegradation in Water and Biodegradation in Zebrafish Embryos (*Danio rerio*). *Environ Sci Technol*. doi: 10.1021/acs.est.9b00789
47. Schymanski EL, Jeon J, Gulde R, Fenner K, Ruff M, Singer HP, Hollender J (2014) Identifying small molecules via high resolution mass spectrometry: Communicating confidence. *Environ. Sci. Technol.* 48:2097–2098
48. Gulde R, Meier U, Schymanski EL, Kohler HPE, Helbling DE, Derrer S, Rentsch D, Fenner K (2016) Systematic Exploration of Biotransformation Reactions of Amine-Containing Micropollutants in Activated Sludge. *Environ Sci Technol* 50:2908–2920 . doi: 10.1021/acs.est.5b05186
49. Ribeiro AR, Afonso CM, Castro PML, Tiritan ME (2013) Enantioselective biodegradation of pharmaceuticals, alprenolol and propranolol, by an activated sludge inoculum. *Ecotoxicol Environ Saf* 87:108–114 . doi: 10.1016/j.ecoenv.2012.10.009
50. Kunkel U, Radke M (2012) Fate of pharmaceuticals in rivers: Deriving a benchmark dataset at favorable attenuation conditions. *Water Res* 46:5551–5565 . doi: 10.1016/j.watres.2012.07.033
51. Nikolai LN, McClure EL, MacLeod SL, Wong CS (2006) Stereoisomer quantification of the β -blocker drugs atenolol, metoprolol, and propranolol in wastewaters by chiral high-performance liquid chromatography-tandem mass spectrometry. *J Chromatogr A* 1131:103–109 . doi: 10.1016/j.chroma.2006.07.033
52. Zirlewagen J, Strathmann M, Schiperski F, Licha T, Nödler K, Hillebrand O, Idzik K (2013) Occurrence and fate of the angiotensin II receptor antagonist transformation product valsartan acid in the water cycle – A comparative study with selected β -blockers and the persistent anthropogenic wastewater indicators carbamazepine and acesulfame. *Water Res* 47:6650–6659 . doi: 10.1016/j.watres.2013.08.034
53. Radjenović J, Pérez S, Petrović M, Barceló D (2008) Identification and structural characterization of biodegradation products of atenolol and glibenclamide by liquid chromatography coupled to hybrid quadrupole time-of-flight and quadrupole ion trap mass spectrometry. *J Chromatogr A* 1210:142–153 . doi: 10.1016/j.chroma.2008.09.060
54. Stravs MA, Pomati F, Hollender J (2017) Exploring micropollutant biotransformation in three freshwater phytoplankton species. *Environ Sci Process Impacts* 19:822–832 . doi: 10.1039/c7em00100b
55. Yin L, Ma R, Wang B, Yuan H, Yu G (2017) The degradation and persistence of five pharmaceuticals in an artificial climate incubator during a one year period. *RSC Adv* 7:8280–8287 . doi: 10.1039/c6ra28351a
56. Kern S, Baumgartner R, Helbling DE, Hollender J, Singer H, Loos MJ, Schwarzenbach RP, Fenner K (2010)

- 533 A tiered procedure for assessing the formation of biotransformation products of pharmaceuticals and
534 biocides during activated sludge treatment. *J Environ Monit* 12:2100–2111 . doi: 10.1039/c0em00238k
- 535 57. Rubirola A, Llorca M, Rodríguez-Mozaz S, Casas N, Rodríguez-Roda I, Barceló D, Buttiglieri G (2014)
536 Characterization of metoprolol biodegradation and its transformation products generated in activated sludge
537 batch experiments and in full scale WWTPs. *Water Res* 63:21–32 . doi: 10.1016/j.watres.2014.05.031
- 538 58. Lv M, Lo C, Hsu CC, Wang Y, Chiang YR, Sun Q, Wu Y, Li Y, Chen L, Yu CP (2018) Identification of
539 enantiomeric byproducts during microalgae-mediated transformation of metoprolol by MS/MS spectrum
540 based networking. *Front Microbiol* 9:1–11 . doi: 10.3389/fmicb.2018.02115
- 541 59. Jaén-Gil A, Castellet-Rovira F, Llorca M, Villagrasa M, Sarrà M, Rodríguez-Mozaz S, Barceló D (2019)
542 Fungal treatment of metoprolol and its recalcitrant metabolite metoprolol acid in hospital wastewater:
543 Biotransformation, sorption and ecotoxicological impact. *Water Res* 171–180 . doi:
544 10.1016/j.watres.2018.12.054
- 545 60. Fono LJ, Sedlak DL (2005) Use of the chiral pharmaceutical propranolol to identify sewage discharges into
546 surface waters. *Environ Sci Technol* 39:9244–9252 . doi: 10.1021/es047965t
- 547 61. Domínguez-Romero JC, García-Reyes JF, Martínez-Romero R, Berton P, Martínez-Lara E, Del Moral-Leal
548 ML, Molina-Díaz A (2013) Combined data mining strategy for the systematic identification of sport drug
549 metabolites in urine by liquid chromatography time-of-flight mass spectrometry. *Anal Chim Acta* 761:1–10 .
550 doi: 10.1016/j.aca.2012.11.049
- 551 62. Conard GJ, Ober RE (1984) Metabolism of flecainide. *Am J Cardiol* 53: . doi: 10.1016/0002-9149(84)90501-
552 0
- 553 63. Kasprzyk-Hordern B (2010) Pharmacologically active compounds in the environment and their chirality.
554 *Chem Soc Rev* 39:4466–4503 . doi: 10.1039/c000408c
- 555 64. Gross A, Mikus G, Fischer C, Hertrampf R, Gundert-Remy U, Eichelbaum M (1989) Stereoselective
556 disposition of flecainide in relation to the sparteine/debrisoquine metaboliser phenotype. *Br J Clin Pharmacol*
557 28:555–566 . doi: 10.1111/j.1365-2125.1989.tb03542.x
- 558 65. De Wildeman SMA, Sonke T, Schoemaker HE, May O (2007) Biocatalytic reductions: From lab curiosity to
559 “first choice.” *Acc. Chem. Res.* 40:1260–1266
- 560 66. An J, Nie Y, Xu Y (2019) Structural insights into alcohol dehydrogenases catalyzing asymmetric reductions.
561 *Crit. Rev. Biotechnol.* 39:366–379
- 562 67. Zhu D, Hua L (2010) How carbonyl reductases control stereoselectivity: Approaching the goal of rational
563 design. *Pure Appl Chem* 82:117–128 . doi: 10.1351/pac-con-09-01-03
- 564 68. Brienza M, Chiron S (2017) Enantioselective reductive transformation of climbazole: A concept towards
565 quantitative biodegradation assessment in anaerobic biological treatment processes. *Water Res* 116:203–
566 210 . doi: 10.1016/j.watres.2017.03.037
- 567 69. Mikuš P, Maráková K, Marák J, Planková A, Valášková I, Havránek E (2008) Direct determination of
568 celiprolol in human urine using on-line coupled ITP-CZE method with fiber-based DAD. *Electrophoresis*
569 29:4561–4567 . doi: 10.1002/elps.200800079
- 570 70. Celiprolol @ drugbank. <https://www.drugbank.ca/drugs/DB04846>. Accessed 3 Sep 2019
- 571 71. De Peuter OR, Souverein PC, Klungel OH, Bller HR, De Boer A, Kamphuisen PW (2011) Non-selective vs.
572 selective beta-blocker treatment and the risk of thrombo-embolic events in patients with heart failure. *Eur J*
573 *Heart Fail* 13:220–226 . doi: 10.1093/eurjhf/hfq176

574

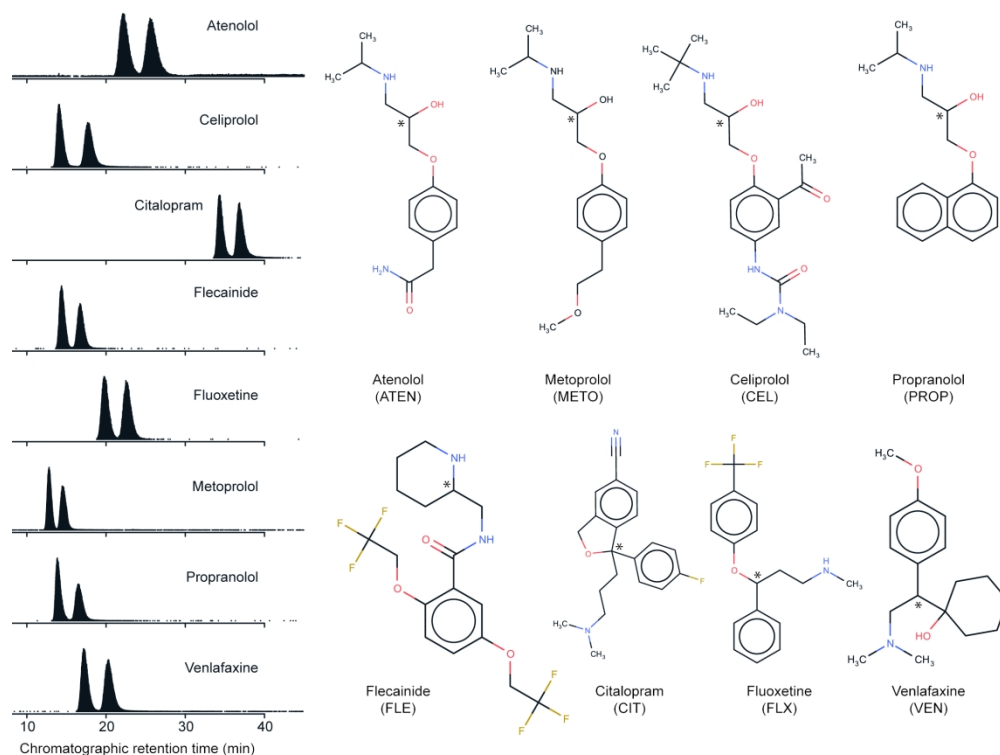


Fig. 1 Eight chiral drugs with constant enantiomeric resolution ($R_s > 1.0$) in NANOpure™ water using method 1 (Table 1). *Left*: extracted ion chromatograms of analytes (sum of enantiomers: $10 \mu\text{g L}^{-1}$, absolute: 0.5 ng , no enrichment).

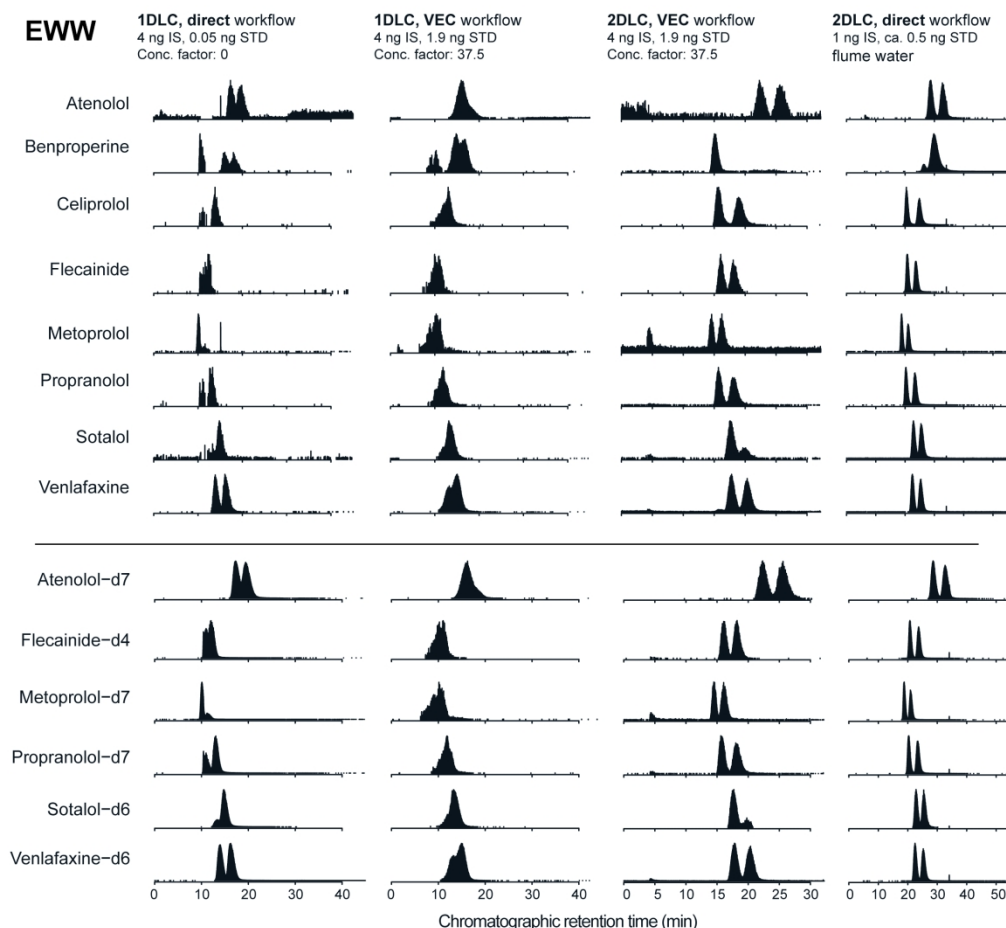


Fig. 2 Loss or decrease of enantiomeric resolution during one-dimensional chiral liquid chromatography (1DLC, 1st and 2nd column, in comparison to NPW in Fig. 1) of racemic analyte standards (STD, top) and assigned racemic isotope-labelled internal standards (IS, bottom) in effluent wastewater (EWW) and EWW concentrated by vacuum-assisted evaporation (VEC) – restoration of enantiomeric resolution through achiral-chiral two-dimensional liquid chromatography (2DLC, 3rd column) and its application to an artificial EWW sample taken from a recirculating water-sediment test flume (4th column). *General notes:* analyte amounts in column header are the sum of both enantiomers; scaling of omitted y-axes can differ; STDs and isotope-labeled internal standards of citalopram and fluoxetine are not shown (for other matrices see Fig. SI.D-8) due to analytical issues; mass traces cut after 50 min in 4th column.

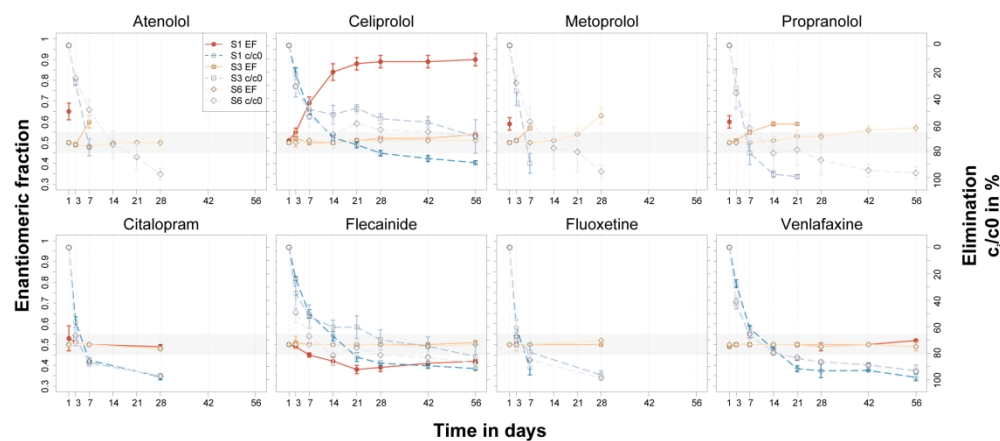


Fig. 3 Enantiomeric fractions (EF, solid lines) and elimination (dashed lines) of 8 chiral organic contaminants over the 56-days experimental period. Treatments differ in sediment dilution (i.e. bacterial diversity; S1, S3, S6). Bedform numbers are not resolved. Contaminants were spiked at racemic composition (EF 0.50 ± 0.05 , grey bar). Data points with error bars: mean \pm SD. The maximum EF over 56 days are summarized in SI.I.

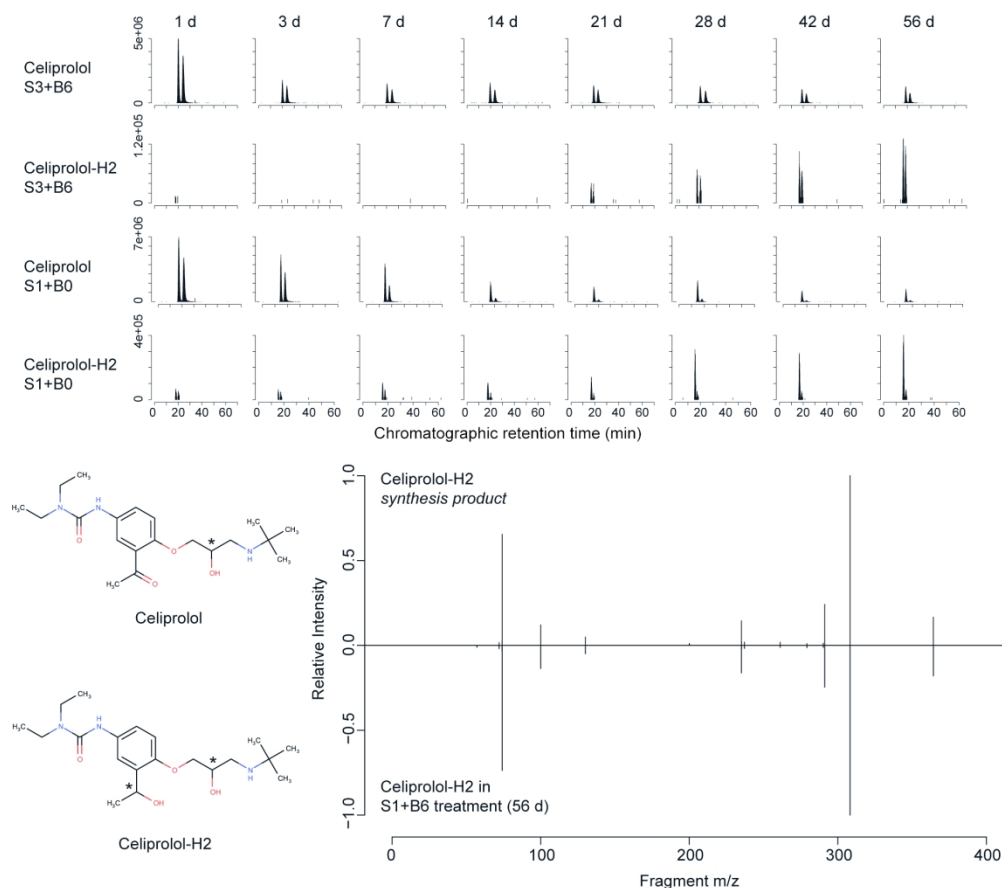


Fig. 4 Evidence for the (biotic) enzymatic reduction of celiprolol to celiprolol-H2. *Top*: Extracted-ion chromatograms (2DLC) of celiprolol and celiprolol-H2 from 1 d to 56 d after fortification. At intermediate bacterial diversity (S3+B6) celiprolol attenuation and celiprolol-H2 formation occur via a non-enantioselective process. At high bacterial diversity (S1+B0), celiprolol undergoes strong enantiomeric fractionation and only 1 dominant celiprolol-H2 peak evolves (please note: the enantiomeric composition of celiprolol-H2 was assessed visually). *Bottom*: head-to-tail plot of ms2 fragments obtained for synthesized celiprolol-H2 and celiprolol-H2 in a S1+B6 flume. 96% similarity between ms2 spectra at 10 ppm mass tolerance and 0.01 relative intensity cut-off (overlap: 14 of 16 fragments).